Hindawi
International Journal of Photoenergy
Volume 2022, Article ID 8149765, 7 pages
https://doi.org/10.1155/2022/8149765

Research Article

Study on Sunshine Stress Effect of Long-Span and Wide Concrete Box Girder

Wang Cheng[1], **Zhang Chentian**[2], **Li Shuo**[3] **and Li Jianhua**[1]

[1]*CCCC Fourth Highway Engineering Co., Ltd., Beijing 100022, China*
[2]*Planning and Construction Bureau of Management Committee Xiong'an New Area, Hebei 071000, China*
[3]*Key Laboratory of HVAC, Beijing University of Civil Engineering and Architecture, Beijing 100044, China*

Correspondence should be addressed to Wang Cheng; 2918769791@qq.com

Received 30 October 2021; Revised 19 April 2022; Accepted 10 May 2022; Published 31 May 2022

Academic Editor: Alberto Álvarez-Gallegos

In order to further clarify the sunshine stress effect of long-span and wide concrete box girder, the study selected a concrete box girder with 4×42 m span and 33.5 m width, formed the temperature field load through a field test and numerical simulation, established a numerical analysis model by using the finite element program of ANSYS, and comprehensively analyzed the longitudinal temperature stress distribution of a long-span and wide concrete box girder under sunshine. The midspan section of the first span of the box girder is selected for field stress measure, and the field measure results and numerical analysis results are compared and analyzed. The research shows that the results of field measurement and numerical simulation are basically consistent. Sunshine temperature has a great influence on long-span and wide concrete box girder, which should be paid enough attention.

1. Introduction

With the rapid urban development, a long-span and wide concrete box girder is more and more widely used. On the one hand, it has greatly improved the urban operation efficiency and quality of life. On the other hand, it puts forward higher requirements for civil engineering technology. A long-span and wide-width concrete box girder is mostly used in outdoor space, such as large bridge structure and public facility structure, which requires high-temperature adaptability [1, 2]. At the same time, due to the complex structure and large temperature distribution gradient, the influence is more significant [3]. In this paper, the sunshine stress effect of long-span and wide concrete box girder is studied in Zhuhai Hengqin second bridge project.

2. Model Establishment

The Hengqin second bridge is located in the southwest of Zhuhai City. Its south approaching bridge is a cast-in-situ concrete box girder with a standard span of 42 m and a width of 33.5 m for the beam top plate and 17.50 m for the bottom plate. The beam height at the center line is 2.5 m, the top plate is 0.25 m thick, and the bottom plate is 0.25 m thick. It is locally thickened near the fulcrum to meet the stress needs of the structure. Figure 1 is the cross-section diagram of the large-span wide concrete box girder.

The longitudinal length of the bridge structure is much larger than the vertical length and transverse length. If the three-dimensional conduction property of temperature in some areas of the bridge structure is ignored, it can be considered that the temperature change of the bridge along the length direction is consistent. So the three-dimensional heat conduction problem can be simplified to analyze the one-dimensional heat conduction state along the transverse and vertical directions of the bridge [4, 5]. Therefore, only one section along the longitudinal direction of the bridge needs to be selected as a representative. The middle of the first span of the first part (4×42 m) is selected as the temperature and stress measure section, as shown in section A in Figure 2.

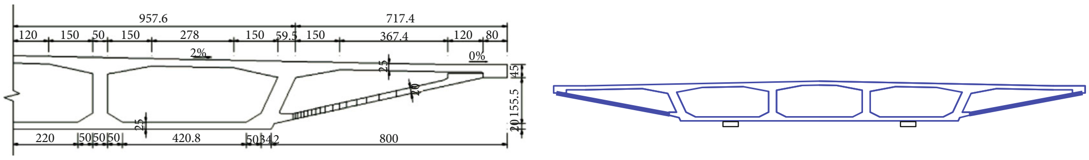

(a) Beam section size

(b) Beam section layout

Figure 1: Cross-section diagram of the large-span wide concrete box girder.

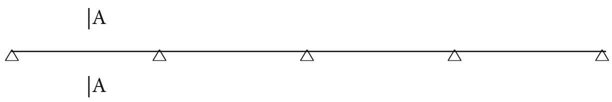

Figure 2: Diagram of the measure section position.

3. Temperature Field Measure

As shown in Figure 2, the temperature measure section is A-A. The temperature sensors are arranged and installed on the upper surface, lower surface, and web of the box girder [6], and the positions are shown in Figure 3.

According to the construction situation of the project, the temperature measure is conducted on a hot day for 24 hours [7]. Figure 4 shows the measured temperature results of the measuring points of the upper surface, lower surface, and web of the box girder within 24 hours.

Under the action of sunshine, the minimum vertical temperature difference occurs at 6 a.m. and the maximum temperature difference occurs at 14 a.m., with a temperature difference value of about 16°C. The transverse temperature difference of the upper surface is relatively uniform, and the maximum temperature difference value is 5°C. The transverse temperature difference of the lower surface is uniform, and the temperature difference value is less than 1°C. The temperature change law of each measuring point changes roughly according to the sinusoidal curve. The internal temperature distribution is uneven, and the temperature of the measuring point near the roof changes greatly during the day.

In order to facilitate engineering application, this study directly uses the field measured temperature value of the boundary as linear interpolation to form the temperature boundary condition of the outer surface of the box girder and then obtains the temperature distribution inside the box girder through steady-state thermal analysis[8, 9]. After the temperature field of the bridge structure is determined, the structural temperature load can be formed according to the thermophysical properties of the material itself [10].

4. Temperature Stress Measure

In order to study the effect of temperature effect, the temperature stress of the box girder is observed while observing the temperature field. The stress measure section of the box girder is the same as the temperature measure section [8], as shown in section A-A in Figure 1.

The layout position of the stress measure sensor is shown in Figure 5. The sensor is bound with the reinforcement and embedded in the structure before concrete pouring.

The measure lasted 24 hours from 14:00 p.m. to 14:00 p.m. the next day. A total of 13 measures were recorded once every two hours. The measure results accurately reflect the change of internal stress of the box girder in one day.

The measure result takes the result at 14:00 at the beginning of the test as the zero point, and the subsequent measure results are the difference from the results at that time. The greater the positive difference, the more it decreases. The greater the negative difference, the more it increases. Therefore, the measured value is not the specific stress but reflects the stress change caused by sunshine temperature [11].

5. Stress Time History Variation

The study selected the solid70 thermal analysis unit provided by ANSYS and ignored the influence of prestressed reinforcement on temperature distribution. The stress distribution of the box girder under the temperature field is calculated and compared with the measured data. The results are shown in Figure 6.

According to the analysis and statistical results of measured and calculated values, under the action of 24-hour solar radiation, the longitudinal compressive stress of the box girder roof gradually decreases with the continuous decrease in temperature. On the contrary, when the temperature rises, the longitudinal compressive stress increases gradually. The variation law and amplitude of measured and calculated values are basically the same, and the maximum error is about 15%. At 14:00 p.m. or 16:00 p.m., the compressive stress at each measuring point of the roof reaches the maximum value. The compressive stress decreases rapidly after dusk and remains at a low level at night and begins to rise rapidly after 8:00 a.m. the next day.

6. Spatial Distribution of Box Girder Stress

6.1. Overall Stress Analysis. Taking 14:00 p.m. with the highest roof temperature and 6:00 a.m. with the lowest temperature difference between roof and floor as examples, Figures 7–14 describe the stress distribution of the roof, lower surface, and the middle section of the first span.

It can be seen from the figure that the roof is subjected to large compressive stress at 14 p.m., the maximum local compressive stress is about 8×10^6 Pa, and the compressive stress of the bottom plate is about 2×10^6 Pa. It can be seen from the midspan section that the middle of the web is under

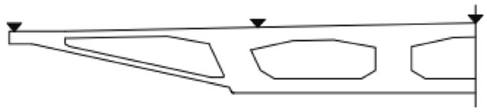

(a) Upper surface (measuring point no.: 1, 2, and 3 from left to right)

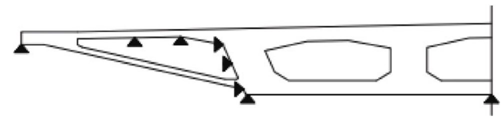

(b) Lower surface (measuring point no.: 4, 5, 6, 7, 8, 9, 10, and 11 from left to right)

(c) Web (measuring point no.: the left side is 12, 13, 14, 15, and 16 from top to bottom;the right side is 17, 18, 19, and 20 from top to bottom)

Figure 3: Layout diagram of beam temperature measuring points.

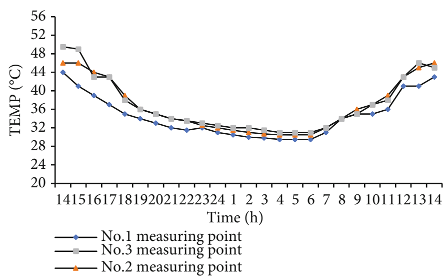

(a) Upper surface

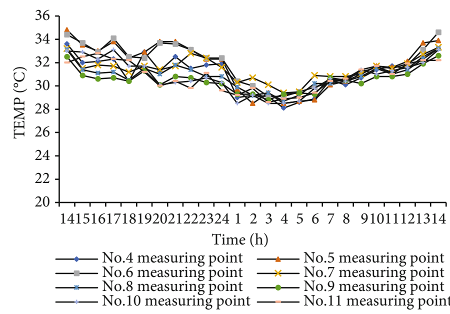

(b) Lower surface

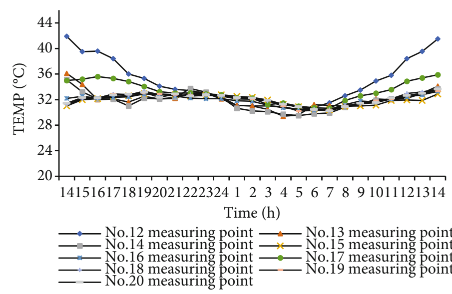

(c) Web

Figure 4: Beam temperature measured results.

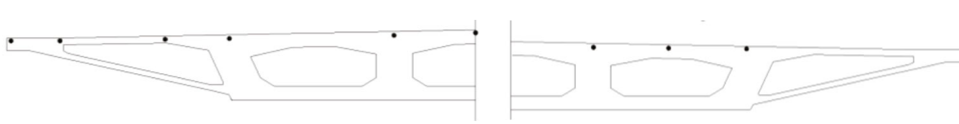

Figure 5: Layout diagram of stress sensor (the horizontal coordinate is 0 at the left end of the cross section).

the action of tensile stress, and there is a large tensile stress at the bottom of the top plate, which is more than 2.5×10^6 Pa. The transverse and longitudinal distribution of stress in the top plate and bottom plate is uneven.

At 6 a.m., the compressive stress value of the top plate is small, the bottom plate is partially compressed and partially tensioned, and the value is small. The horizontal and vertical distribution of the stress in the box is relatively uniform.

6.2. Analysis of Transverse Distribution of Roof Stress. According to the time history stress analysis, the maximum stress of the roof and the maximum vertical stress gradient appeared at 14 p.m.

Figure 15 shows the calculation results of transverse distribution of longitudinal stress of roof at 14 p.m. It can be seen from the results that the roof is in compression, and the longitudinal compressive stress in the middle is the largest, about 8.4×10^6 Pa. The transverse distribution of stress is "V" shape as a whole, and the stress decreases gradually from the middle of the section to both sides.

The main reasons for the uneven transverse distribution of stress are as follows: (1) the shear lag effect of the box girder reduces the longitudinal stress of the cantilever section and (2) the difference of stiffness between the middle and both sides of the roof leads to the difference of transverse stress distribution [12].

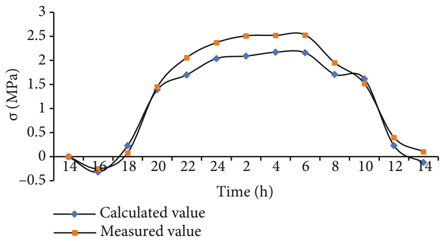

(a) No. 1 measuring point

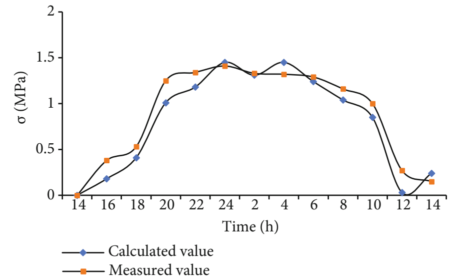

(b) No. 2 measuring point

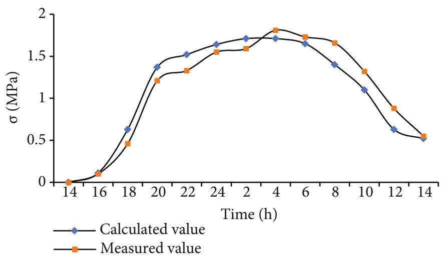

(c) No. 3 measuring point

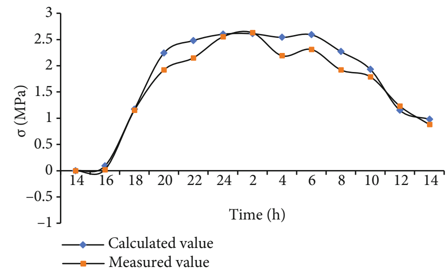

(d) No. 4 measuring point

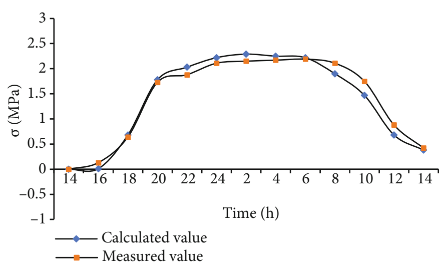

(e) No. 5 measuring point

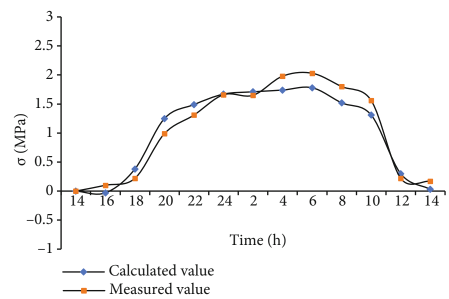

(f) No. 6 measuring point

FIGURE 6: Time history diagram of temperature stress comparison.

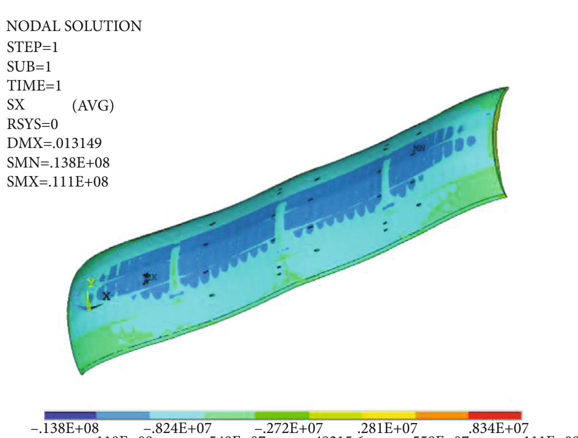

FIGURE 7: Longitudinal stress distribution at 14 (roof)/Pa.

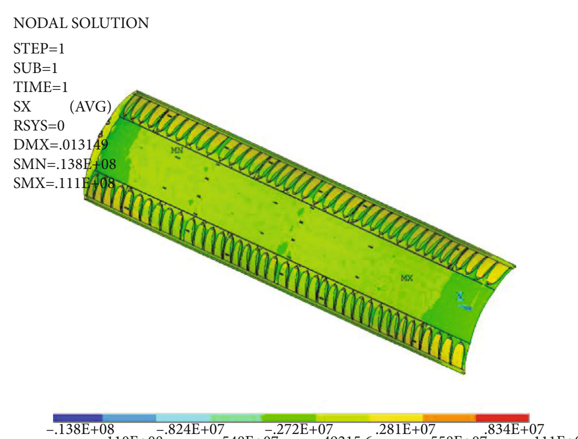

FIGURE 8: Longitudinal stress distribution at 14 (lower surface)/Pa.

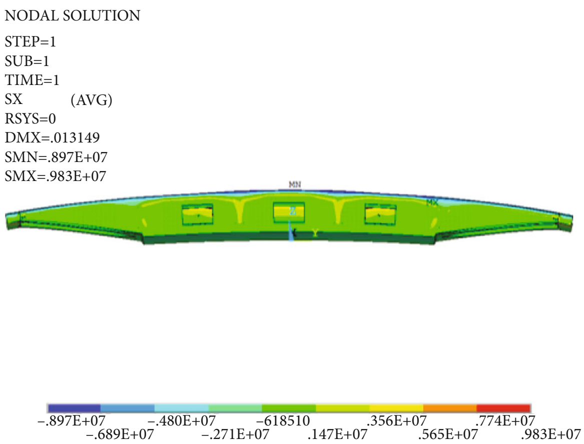

Figure 9: Longitudinal stress distribution at 14 (middle of the first span)/Pa.

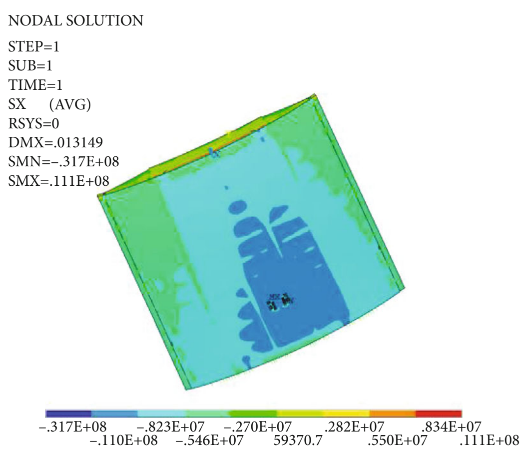

Figure 10: Longitudinal stress distribution at 14 (roof of the first span)/Pa.

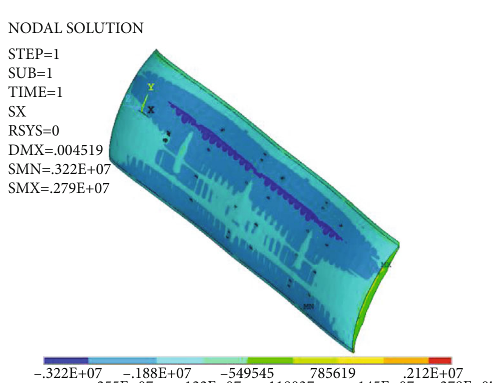

Figure 11: Longitudinal stress distribution at 6 (roof)/Pa.

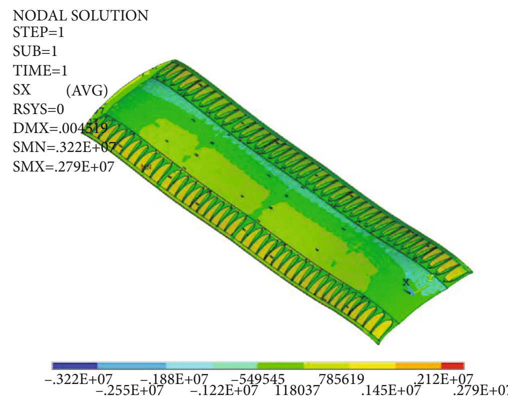

Figure 12: Longitudinal stress distribution at 6 (lower surface)/Pa.

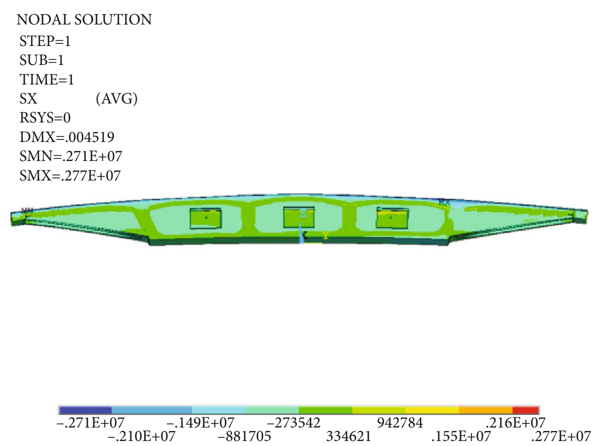

Figure 13: Longitudinal stress distribution at 6 (middle of the first span)/Pa.

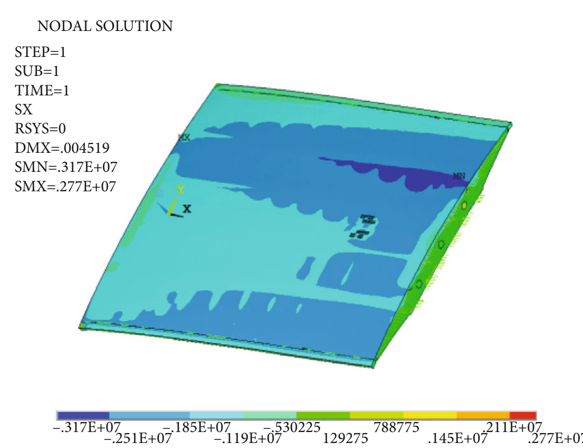

Figure 14: Longitudinal stress distribution at 6 (roof of the first span)/Pa.

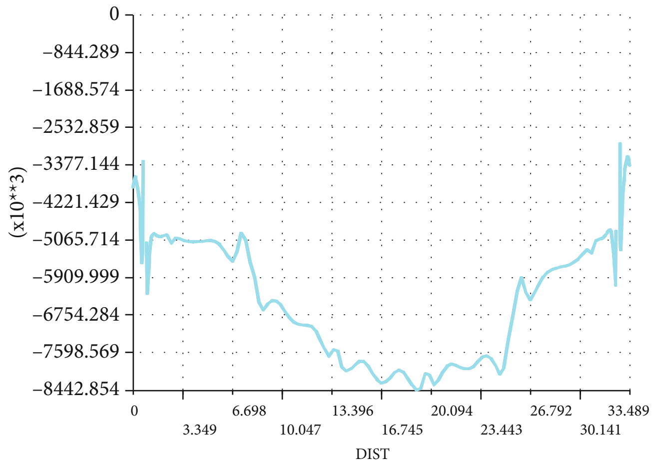

Figure 15: Longitudinal stress distribution of the roof (the ordinate is stress (Pa); the abscissa is distance (m)).

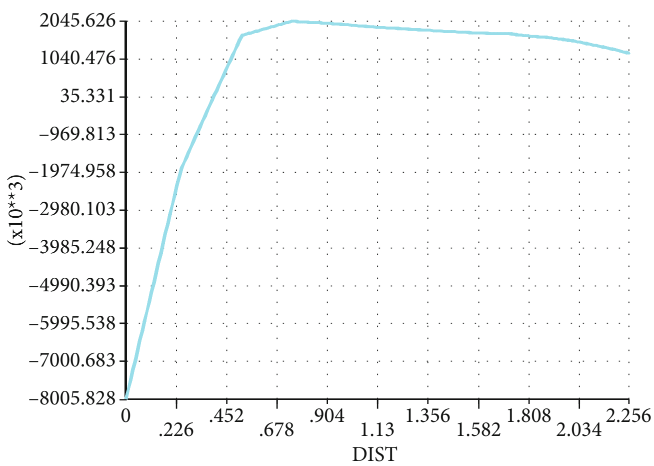

Figure 16: Vertical distribution of longitudinal stress of the web in the middle of the first span (the ordinate is stress (Pa); the abscissa is the distance from the top plate (m)).

6.3. Vertical Stress Distribution of the Box Girder. As can be seen from Figure 16, the compressive stress decreases rapidly with the increase in the distance from the top plate, and the maximum tensile stress appears at the web, which is about 2×10^6 Pa. The critical height point from compressive stress to tensile stress is 30 cm away from the top plate.

7. Conclusion

(1) Based on the field measure and numerical simulation, the time history variation of box girder stress and its uneven spatial distribution are analyzed. Result shows that the simulated value is basically consistent with the measured value, and the maximum error is about 15%. The numerical simulation method is more practical

(2) At 14 p.m., the compressive stress on the top plate of the box girder is large and unevenly distributed, the maximum value of local longitudinal compressive stress is about 8×10^6 Pa, and the stress of the bottom plate is about 2×10^6 Pa. It is necessary to strengthen the structural protection management in different periods of the project site

(3) The transverse distribution of the longitudinal compressive stress of the roof is in a "V" shape as a whole, and the stress decreases gradually from the middle of the section to both sides

(4) The middle and top of the box girder web are subjected to tensile stress. The longitudinal tensile stress at the top of the web is large, exceeding 2.5×10^6 Pa

In short, the sunshine radiation, especially in the case of superimposed dynamic and static loads, has a great impact on the long-span and wide concrete box girder, which should be paid enough attention in the process of design, construction, and use.

Data Availability

The data used to support the findings of this study are available from the corresponding author upon request.

Conflicts of Interest

The authors declare that they have no known competing financial interests or personal relationships that could have appeared to influence the work reported in this paper.

Acknowledgments

The authors are grateful to the financial support of the Scientific Research Program of Beijing Municipal Education Commission (Grant No. KM201910016011) and the Beijing Municipal Natural Science Foundation (3151001).

References

[1] S. Yaqiong and Z. H. Zuo-zhou, "Real-time separation of temperature effect on dynamic strain monitoring and moving load identification of structure," *Engineering Mechanics*, vol. 36, no. 2, pp. 186–194, 2019.

[2] Z. Jianrong, Z. Yuanqiang, L. Jianping, and Z. Zhiyan, "Solar radiation affection on concrete box girder temperature effect," *Journal of Tongji University*, vol. 36, no. 11, pp. 1429–1484, 2008.

[3] W. Gao-xin, D. You-liang, L. Ai, and Z. H. Guang-dong, "Characteristics of transverse temperature differences of steel box girder in run yang cable-stayed bridge using long-term monitoring," *Engineering Mechanics*, vol. 30, no. 1, pp. 163–167, 2013.

[4] L. Yaozhi and D. Shilin, "Mechanical behavior and system changing of cable-truss structures," *Spatial Structures*, vol. 8, no. 4, pp. 45–53, 2002.

[5] L. Yang and W. Z. Y. Yongbin, "Sequentially coupled thermal stress analysis of the prestressed concrete box girder," *Concrete*, vol. 32, no. 10, pp. 139–143, 2015.

[6] L. Lu Jinyu and Q. X. Ding, "Elasto-plastic buckling analysis of novel origami-inspired steel plate shear wall with two-side connections," *Advanced Engineering Sciences*, vol. 50, no. 6, pp. 8–14, 2018.

[7] L. Yong-jian, L. Jiang, and Z. Ning, "Review on solar thermal actions of bridge structures," *China Civil Engineering Journal*, vol. 52, no. 5, pp. 59–78, 2019.

[8] Q. Juntao, Y. Chen, Z. Feng, and L. Xiaoyan, "Study of temperature effect on the composed bridge with corrugated steel webs," *Highway*, vol. 61, no. 3, pp. 54–57, 2016.

[9] D. O. N. G. Xu, D. E. N. G. Zhen-quan, L. I. Shu-chen, G. U. Shou-fa, and Z. H. A. N. G. Feng, "Research on sunlight temperature field and thermal difference effect of long span box girder bridge with corrugated steel webs," *Engineering Mechanics*, vol. 34, no. 9, pp. 230–238, 2017.

[10] J. Vacha, P. Kyzlik, I. Both, and F. Wald, "Beams with corrugated web at elevated temperature, analytical and numerical models for heat transfer," *Fire Safety Journal*, vol. 86, no. 11, pp. 83–94, 2016.

[11] China National Standard, *General Specification for Design of Highway Bridges and Culverts (JTG D60)*, CCCC Highway Planning and Design Institute Co., Ltd., Ed., China Communications Press, 2015.

[12] Chinese National Standard, *Load Code for the Design of Building Structures (GB 5009)*, China Academy of Building Research, Ed., China Construction Industry Press, 2012.